BULETINUL INSTITUTULUI POLITEHNIC DIN IAŞI
Publicat de
Universitatea Tehnică „Gheorghe Asachi” din Iaşi
Volumul 64 (68), Numărul 4, 2018
Secţia
CONSTRUCŢII. ARHITECTURĂ

ENERGY ABSORPTION IN FUNCTIONALLY GRADED CONCRETE UNDER COMPRESSION

BY

TRAIAN-NICU TOADER[1,2,*], WALTER HAASE[1] and WERNER SOBEK[1,3]

[1]Institute for Lightweight Structures and Conceptual Design (ILEK),
Stuttgart Universität, Stuttgart, Germany,
[2]Technical University of Cluj-Napoca
Department of Structures,
[3]Werner Sobek Group, Stuttgart, Germany

Received: October 8, 2018
Accepted for publication: November 16, 2018

Abstract. Functionally graded concrete building components exhibit a density variation of the inner structure in accordance to the stresses that occur locally under load. Such building components are meant to have similar load bearing capacity, lower mass and higher performances for energy dissipation compared to those made of homogeneous distributed normal weight concrete. For the specimen preparation of graded concrete samples two production methods were used: casting and dry spraying. The purpose is to understand the relation between the alternation of concrete layers with various densities and the amount of energy absorbed. To evaluate the energy absorption capacity, cubes of equal mass but with different gradation layouts have been tested against uniaxial compression forces. Results show that the compressive strength and the amount of energy absorbed for the tested functionally graded concrete cubes is influenced by the layout design as well as by the production technique.

Keywords: graded materials; normal weight concrete; lightweight concrete; compression test; concrete failure behaviour.

[*]Corresponding author: *e-mail:* toaderniku@yahoo.com

1. Introduction

Energy absorption in concrete is of interest where there is the possibility of impact loading in the predictable service life of a concrete structure. Wide ranges of situations exist where structures may be subjected to extreme actions such as vehicle impact, derailed trains or earthquakes (Klang *et al.*, 2016).

The presence of various types of microcracks, air voids in the concrete system and pores in the hardened cement paste are weak zones which could initiate the growth of cracks, lowering impact strength. Generally, impact strength of concrete increases with an increase of compressive strength of the concrete material. Concrete with higher compressive strength results in lower energy absorption of the specimen action before cracking (Green, 1964).

An ideal energy absorbing material should have a low crushing strength and capacity for large deformation. During collision kinematic energy is absorbed by crushing the impacted material (Ravindrarajah and Lyte, 2007).

Bischoff *et al*. (1989) made investigations upon energy absorption of concrete incorporating expanded polystyrene beads and reported that this concrete did exhibit similar properties to an ideal energy absorbing material. Compressive strength of concrete samples tested thereby ranged from 4 to 16 MPa. The static tests showed that once peak load was reached, large deformation followed while the load remained constant. Once concrete became compacted under the static load, the load increased until failure, showing a strain hardening effect. Polystyrene aggregate concrete did not fail by cracking which occurs in standard concrete but rather exhibited localized crushing under the head of the force impactor of the samples (Ravindrarajah & Lyte, 2007) , (Bischoff *et al*., 1989).

Under uniaxial compression, dense solid materials such as standard concrete, rocks, ceramics, and ice exhibit progressive distributed damage. These materials fail by slip on inclined shear bands or by axial splitting, or by a combination of both (Bažant & Ožbolt, 1992). On the other hand, porous solid materials such like lightweight concrete, when subjected to uniaxial compression suppress the compressive crushing failure, exhibiting a shearing failure (Huang & Huang, 2000).

Lightweight concrete such as cellular concrete is used for energy absorption in mine support systems replacing the timber. On airports runways different density cellular concrete blocks are used in the arrester beds at the end of runways to catch overrunning planes where the distant limits cannot be met. In these applications the concrete structures not only act as load bearing elements but by undergo compaction when higher loads are applied also fulfill requirements of energy absorbance.

Functionally graded concrete (FGC) enables structural engineers to reduce the structural dead load making it possible to gain lighter building components and to reduce the amount of the required reinforcement. In prefabrication, FGC also makes it possible to reduce the placement and transportation costs. At the Institute for Lightweight Structures and Conceptual Design at the University of Stuttgart, FGC is prepared as a mix of normal weight concrete (NWC) and lightweight aggregate concrete (LWC).

2. Experimental Investigations

2.1. Material Properties

For the production of FGC specimens the two reference mixtures were used: normal weight concrete and lightweight aggregate concrete. The first reference mixture was prepared using cement (CEM I 52.5 R), sand (with aggregate size of 0-2 mm) and water. For the second reference mixture expanded glass as lightweight aggregates partially replaced the sand. The expanded glass granules are spherical. They have a closed surface and sizes of 1-2 mm in diameter (loose bulk density 220 kg/m^3, particle density 350 kg/m^3, crushing resistance 2.4 N/mm^2). For obtaining the graded mixtures, NWC and LWC were combined in different mass ratios (%NWC/%LWC) resulting three new mixtures namely 60/40, 40/60 and 20/80. Table 1 summarizes the mean density, mean strength and amount of energy absorbed determined on cubes made of a single reference mixture respectively, a single graded mixture.

Table 1

Mean Density (ρ_m), Mean Compressive Strength (σ_{cm}) and Amount of Energy Absorbed Determined on Monolithic (single layer) Cubes with a 100 mm Side Length of the Five Concrete Mixtures used and the Two Production Procedures

Properties	Production technology	% NWC / % LWC				
		100/0	60/40	40/60	20/80	0/100
Mean density ρ_m, [kg/m^3]	casting	2,056	1,575	1,335	1,094	854
	dry spraying	2,160	1,728	1,511	1,295	1,079
Mean compressive strength σ_{cm}, [N/mm^2]	casting	50.2	23.8	9.7	4.7	2.6
	dry spraying	43.0	24.9	13.2	10.4	7.8
Energy absorbed per volume unit [J/cm^3]	casting	0.45	0.41	0.65	0.73	0.52
	dry spraying	n/a	1.07	1.23	0.98	1.22

The production technics used in the sample preparation were casting and dry spraying. First technique consists in preparing the two reference mixtures: NWC and LWC as a fresh concrete and deriving from these ones the homogenous graded mixtures were prepared. In the second production technique, the graded mixtures were prepared starting from the dry constituents (cement, sand, expanded glass) which are sprayed from two nozzles with water added to the spray jet. The mixing of the two concrete types is carried out in the spray jet. Layers of 5 mm up to 30 mm in thickness are thereby placed on top of each other to create the specimens. This way the final concrete layer is less homogeneous compared to the casting technique and the thickness of each layer is constrained to multiple of 5 mm. Because of the difference in the concrete production process, the mechanical properties as well as the compressive failure behaviour of the specimens with similar layouts are not the same.

2.2. Details of Specimens

Functionally graded concrete cubes having five and six layers in sequence with similar overall density, as shown in Fig. 1, were tested for flat-wise compression properties using a 500 kN compression test machine. The flat-wise testing procedure involves applying the force perpendicular to the layers, while in the edge-wise testing set up the force is acting parallel to the layers. Previous investigations at the Institute for Lightweight Structures and Conceptual Design performed on FGC cubes showed an increase of 40% of the

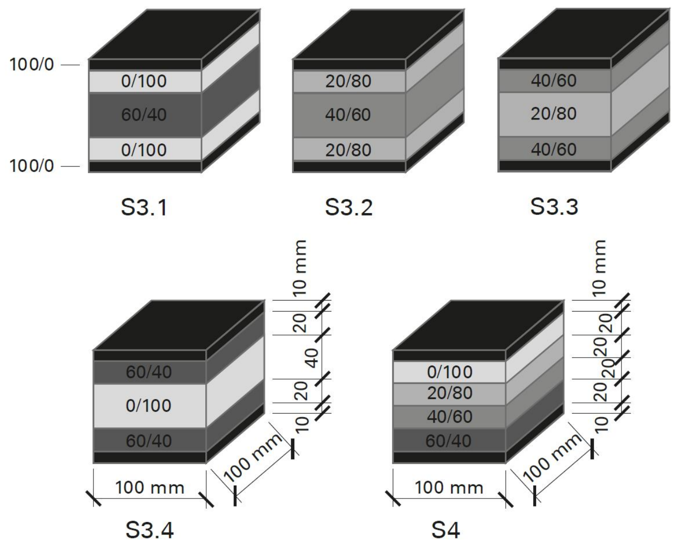

Fig. 1 − Pictorial representation of different FGC cube configurations used in this study.

energy absorbed for the flat-wise compared to the edge-wise compression tested specimens with similar layouts (Toader *et al*., 2017). Therefore the present investigation is focused on the flat-wise compression properties. Four out of five configurations are kept symmetric in order to keep the alternation of layer density variation bond effects minimal. The performances of the designed layouts were investigated for each of the production methods. The testing procedure used was path-controlled with a speed of 1.5 mm/s.

3. Experimental Investigations

3.1. Failure Process

Generally, failure of NWC starts from the interfacial transition zone (ITZ), and no failure in aggregates is found on the fracture surface. The failure under compression displays a steep diagonal cone shape due to shear failure of materials as expected. The failure is composed of initial ITZ cracking and its propagation on paste (Yoon *et al*., 2015). In literature this behaviour is called compressive axial splitting (Hasan *et al*., 2013). Because of their great porosity, lightweight aggregates have less strength and are more deformable than normal weight aggregates. The weakest component of LWC is not the cement matrix or the interfacial transition zone but the lightweight aggregates (Chi *et al*., 2003). Consequently the mechanical performances of FGC specimens are not only controlled by the cement matrix quality but also by the lightweight aggregate volume in concrete and the aggregates properties.

It is observed that, under a constant vertical displacement speed of 1.5 mm/s, all tested specimens failed by cracking or by local crushing of the layers with the highest amount of lightweight aggregates. Each type of the specimens tested against axial compression shown a dominant failure behaviour. Two types of failure processes could be identified in accordance to the propagation of cracks. Representative to the failure of dry sprayed cubes (all 5 layouts) as well as for the cast cubes with a S3.1, S3.2 and S4 layout is the crack pattern with vertical and inclined cracks, Fig. 2. As the compressive strains increased, the number of cracks grew and, simultaneously, the crack openings enlarged. Finally, for each specimen inclined fracture surfaces can be noticed. Due to the spallation of the lateral sides the remaining cube core has an hour-shape. The stress-strain diagram is characterized by a shape similar to the NWC given in the norms (CEN, 2004), but the strains are roughly 10 times larger, Fig. 4 *a*. Each specimen exhibit a single peak stress and the pre-peak deformation was always less than the post-peak one. The second type of failure process is representative for the cast cubes with an S3.3 and S3.4 layout. This time, the first cracks were horizontal and, as predicted, they appeared in the lower density concrete layers. The weakest layer is being crushed while the ones with a higher strength remain undamaged. The cracking extends throughout the entire weak layer before the fracture propagates in the rest of the concrete cube, Fig. 3. The stress-strain diagram has multiple peaks under large deformations, Fig. 4 *b*. The failure is namely cascade graceful behaviour (Klang *et al*., 2016). The failure behaviour of all the layouts is characterized by unexpected large deformations.

Fig. 2 − Representative failure stages of dry sprayed FGC cubes and of S3.1, S3.2 and S4 cast cubes (a dry sprayed specimen with a S3.3 layout is shown).

Fig. 3 − Representative failure stages for FGC cast cubes with an S3.3 and S3.4 layout (a cast specimen with a S3.4 layout is shown).

3.2. Failure Modes

In uniaxial compression tests, two typical stress-strain curves for FGC specimens were observed and illustrated in Fig. 4. Two different failure modes for FGC specimens were also seen and shown in Fig. 5. A compressive axial splitting failure corresponding to the stress-strain curve in Figure 4a occurs for all dry sprayed specimens as well as for those cast with a S3.1, S3.2 and S4 layout. The second failure mode corresponds to the stress-strain curve shown in Fig. 4 *b*, is representative for the cast specimens with a S3.3 and S3.4 layout and it is named compressive crushing failure. The stress-strain curves are generated upon the force-deformation curves considering the area of the undamaged cross section.

Compressive axial splitting failure is specific to NWC subjected to uniaxial compression. Due to the concrete compressive strength – tensile strength ratio of ≈10 and due to its brittle behaviour, when subjected to compression the concrete cubes fail because of the bursting forces which exceeded the tensile strength of the material (CEN, 2004), (Bažant, 2002). Unlike NWC, LWC exhibits a compressive crushing failure, therefor FGC specimens with layers of 0/100 and 20/80 and a thickness of 40mm are characterized by such a type of failure behaviour. On the opposite, in the case of specimens with LWC layer thicknesses of 20 mm or less, the compressive axial splitting failure becomes the dominant one.

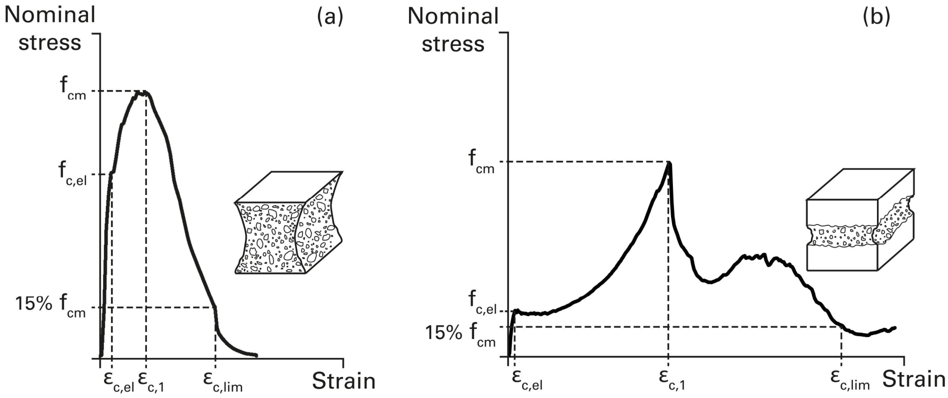

Fig. 4 − Two typical stress-strain curves for FGC cubes in uniaxial compression test (*a*) compressive axial splitting failure (*b*) compressive crushing failure

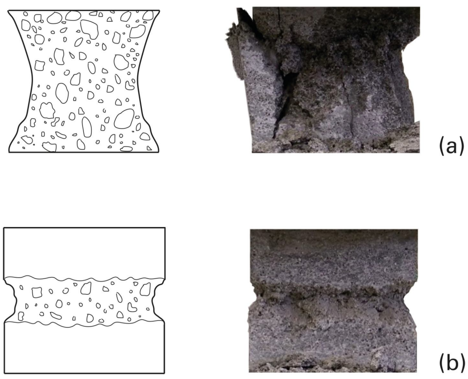

Fig. 5 − Two typical failure modes for FGC cubes in uniaxial compression tests (*a*) compressive axial splitting failure (*b*) compressive crushing failure.

4. Analysis and Discussions of Experimental Results

4.1. Compression Strength

The force-deformation graphs obtained from flat-wise compression testing of FGC are shown in Figs. 6 and 7. The repeatability noticed in three different specimens of each layout type and each production method is also shown in Figs. 6 and 7. It is observed that the scattering in the force-deformation graphs is fairly small. Average compressive strength and energy absorption was determined and data is presented in Table 2 for each layout, based on the force-deformation graphs. Energy absorption values of each layout are evaluated by calculating the area under the force-deformation plot.

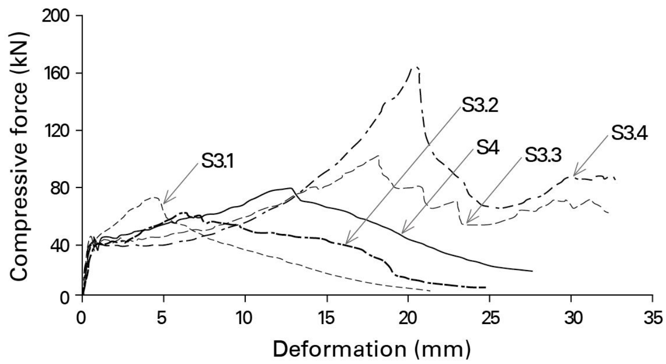

Fig. 6 – Force-deformation plots of cast FGC configurations.

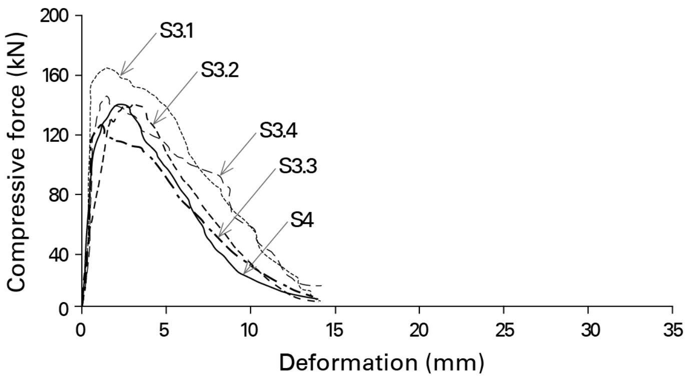

Fig. 7 – Force-deformation plots of dry sprayed FGC configurations.

The strength of FGC cubes (Table 2) is significant higher compared with the strength of weakest (lowest density) layer determined on monolithic (single layer) concrete cubes (Table 1). For instance the weakest layer for the configurations S3.1, S3.4 and S4 is 0/100 and has a strength of 2.6 MPa when cast and 7.8 MPa when dry sprayed, while the strength of the FGC configurations is 6.2,...,15.7 MPa, respectively 13.8,...,17.0 MPa. For the configurations S3.2 and S3.3 the weakest layer is 20/80 and has a strength determined on cubes of 4.7 MPa when cast and 10.4 MPa when dry sprayed, by contrast the FGC specimens shown a nominal strength of 6.9,...,9.9 MPa, respectively 11.0,...,12.5 MPa.

Table 2

Compressive Properties of Cast and Dry Sprayed FGC Configurations

Type of FGC specimen	Density (kg/m^3)		Average compressive strength (MPa)		Energy absorption (J/cm^3)	
	cast	dry sprayed	cast	dry sprayed	cast	dry sprayed
S3.1	1497 ± 88	1623 ± 76	9.2	17.0	1.44	1.13
S3.2			6.9	12.5	0.70	0.83
S3.3			9.9	11.0	1.63	0.74
S3.4			15.7	13.8	2.29	1.04
S4			6.2	14.0	1.05	0.81

Comparing the force-deformation plots in Figs. 6 and 7, a clear distinction can be made in between the behaviour of cast and dry sprayed specimens. Under compression a linear behaviour is experienced until a roughly 4 MPa limit is reached for the FGC cast cubes, respectively 10 MPa for the dry sprayed ones. Based on the values given in Table 2 the average compressive strength of the FGC cubes is mostly higher when the dry spraying technology is used. The difference in compressive strength can be attributed to the difference in layer production and bonding between the two fabrication methods.

From Fig. 6 and Table 2, it is also found that all force-deformation plots of symmetric FGC cast configurations do not follow a similar trend. Symmetric configurations as S3.1 and S3.4, or S3.2 and S3.3 exhibit different strengths and deformation capacities. It is observed that the force-deformation curves obtained for all FGC cast configurations increased until elastic limit was reached, corresponding to deformations of 1 mm or less. The point coincides to the stress level where the cracks spread and increased in width inside the weakest layers, 0/100 and 20/80, leaving the stronger layers, 60/40 and 40/60 undamaged. Further, for configurations S3.1, S3.2 and S4, the curve slope increased until reaching a consolidation point, matching this way the maximum strength of the specimen. Afterwards, the deformation was increased further on and the strength declined until total deformations of 20 mm or more were measured, in the limit of maximum 85% strength loss. On the other hand, for configurations S3.3 and S3.4, on the force-deformation plot the linear trend was followed by an almost flat trend for 4 mm up to 8 mm deformation. Furthermore the strength started to increase rapidly towards reaching the first consolidation point, matching this way the maximum strength of the specimen. The deformation continued to be increased further under constant speed and the strength of the specimen decreased and increased back again several times before the limit of 85% strength loss was reached. By partially regaining their strength the specimens show large deformations of up to 50 mm and therefore the force-deformation curves are characterized by a multitude of peaks. Specific to all FGC cast configurations is the crack propagation into the stronger layers initiated only after the first peak on the force-deformation diagram was reached.

From Fig. 7 and Table 2, it is found that force-deformation plots of symmetric FGC dry sprayed configurations follow a similar trend with differences in the strength. Symmetric configurations as S3.1 and S3.4, or S3.2 and S3.3 as well as the unsymmetrical configuration S4, exhibit similar deformation capacity and compression behaviour. The force-deformation curves of the FGC dry sprayed specimens followed a more smother curve than the FGC cast ones. Qualitatively speaking, the force-deformation curves of all the FGC dry sprayed specimens followed the shape of the regular NWC cubes but with having the deformations scaled up almost 10 times.

In order to emphasize on the concrete mixture type and layer sequencing effect of the compression properties for the studied concrete cubes, force-deformation plots for cast FGC (S3.4 configuration), NWC, LWC, and concrete mixtures 60/40, 40/60, respectively, 20/80 are compared to one another and shown in Fig. 8. Unlike NWC cubes, specific to the FGC ones is that the maximum compression force is reached only after the weak layers were damaged. From this figure it can be noticed that NWC cubes have higher strength but deformations of less than 1 mm. They are then followed by the

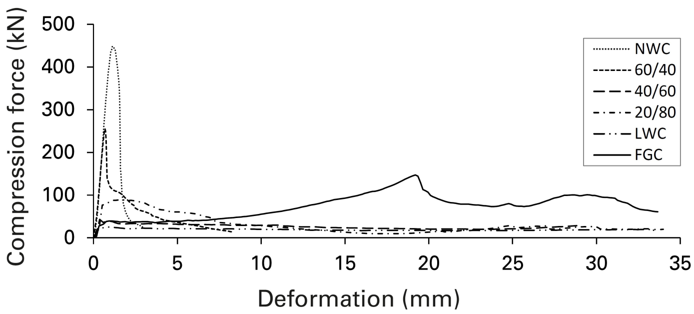

Fig. 8 – Force-deformation plots comparison of cubes made of cast NWC, LWC, various concrete graded mixtures and FGC.

cubes made of plain concrete mixtures 60/40 and 40/60 which decrease in strength to less than half of NWC's strength (50.2 MPa) but they gain a deformability of over 10 times larger. The monolithic 20/80 concrete cubes and the monolithic LWC cubes are the first to exhibit a deformation capacity of more than 35 mm. However, both layouts with 20/80 and LWC experience a drastically strength reduction of 10 times smaller respectively, 20 times smaller, than the cubes made of NWC. Once the transition towards FGC is made, the cubes large deformability can be kept and a strength of 15.7 MPa can be assured by using the S3.4 configuration, which represents approximately one third of the NWC strength.

4.2. Energy Absorption

An important parameter for materials under compressive stresses is the energy absorption. The amount of energy absorbed by a specimen is obtained by evaluating the integral of the force-deformation curve. Due to the large deformations of FGC cubes, even though the maximum compression stress is considerable lower than the one of NWC, the amount of energy absorbed is several times higher, Fig. 9. Furthermore, if one takes into consideration the ratio between the energy absorbed and the specimen`s weight it becomes even more obvious that the FGC has a much higher specific energy absorption then NWC.

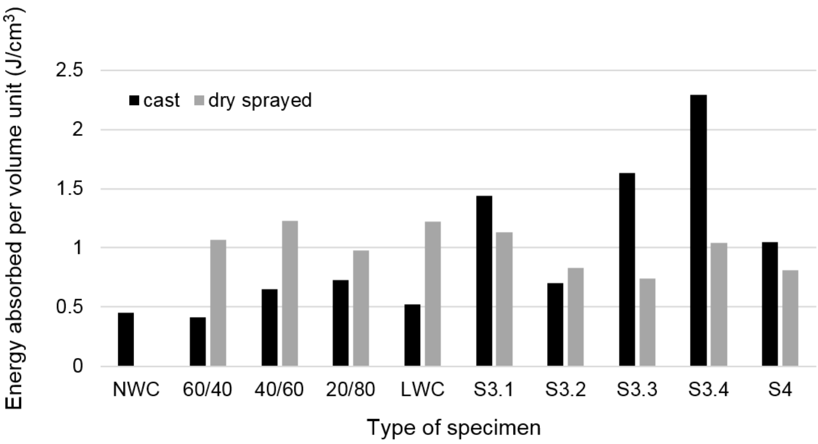

Fig. 9 – Bar chart representation of energy absorption in NWC, LWC, concrete graded mixtures and FGC per cm^3 when subjected to uniaxial compression.

The amount of energy absorbed in the FGC dry sprayed configurations is lower than the one in the monolithic (single layer) graded mixture concrete cubes. On the other hand, for the FGC cast configurations the amount of energy absorbed is at least two or three times higher than the one in the monolithic graded mixture concrete cubes. It is also found that the energy absorption values in FGC cast configurations S3.3 and S3.4 are higher compared to their counter configurations. In addition, the FGC with central low-density layers arrangements are structurally more stable. It is obvious that the failure of structures always initiate at the weakest point. Therefore, the configurations with single weakest layer at the centre have more localized failures. On further loading the micro-localized failures become macro-failures but without crack propagation in the stronger layers. Only after the weakest layer was completely crushed the cracks are propagating towards stiffer layers, respectively due to which the FGC specimen keeps his volumetric integrity for long paths. On the other hand, the FGC cast configurations with central denser layer arrangements are structurally less stable due to the larger number of localized failures. This causes a more rapid crack propagation towards the stiffer layers and therefore a sooner disintegration of the concrete specimen. Thus, it is evident that compression and energy absorbance properties of FGC are affected by the layer sequencing.

4.3. Compression Failure Prediction Using Nonlinear Finite Element Analyse

The designed and developed FGC configurations were further analyzed for cracking and failure behavior using finite element software Atena 3D. Each configuration was modelled as a cube with a size of 100 mm using twenty-node brick elements and a mesh size of 10 mm. The material was defined as a “3D nonlinear cementitious 2” type existing in the software`s library, which is suitable for concrete like materials and has the advantage of being a fully incremental model (both the plastic part as well as the fracturing part). For defining the contact between the layers a perfect connection was chosen, in accordance to the continuous production process and to the observations during the experimental campaign when no slip between layers was noticed. The used nonlinear solvers are standard Newton-Raphson and standard Arc Length based.

The numerical simulations show a good predictability of the cracking and failure behaviour, Fig. 10. To emphasize on the differences between the two types of failure, compressive axial splitting failure and compressive crushing failure are shown in opposition. A representative concrete cube layout corresponding for each type of failure was modelled and analyzed using the finite element method. Therefore two extreme specimens can be seen in Figure 10, the NWC cube specimen which can be considered representative for ordinary normal strength concrete, and the FGC cube specimen with a S3.4 layout for which the highest energy absorption value was recorded.

For the NWC cube specimen vertical cracks started to develop in the areas close to the vertical edges. Simultaneously with increasing the vertical deformation, the cracks propagated towards the center of the cube keeping a vertical trend and increased in width up to 0.78 mm. The failure behaviour of the cube under uniaxial compression forces was similar with the one during the physical experiments.

Numerical simulation performed on the FGC S3.4 configuration showed an identical development and propagation of the cracks as in the experiment. Localized failure material can be also seen in Figure 10. Here large inclined and almost horizontal cracks appear in the weak layer, all showing a material crushing failure. In the end the failure behaviour of the FGC cube had a very good match with the one throughout the experimental campaign. An important parameter for materials under compressive stresses is the energy.

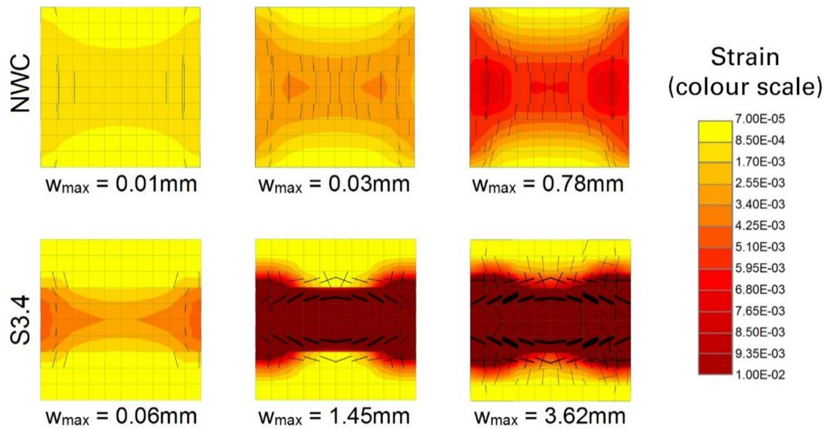

Fig. 10 – Cracking behaviour and lateral strain state in finite element analyse for cast cubes made of NWC and FGC (S3.4 layout) subjected to uniaxial compression.

5. Conclusions

The investigations show an increase of the energy absorption in the FGC cubes compared to NWC ones by up to 408%, compared to LWC by 88÷340%, and in contrast to monolithic graded mixture concrete cubes increased in the range of 86,...,459%.

The deformation capacity of FGC specimens compared to NWC ones is increased up to 20 times. The cast specimens compared to the dry sprayed ones with similar layout show comparable strength, an improvement of up to 3 times in deformation capacity and approx. double energy absorption value.

The FGC cast configuration S3.4 exhibited higher compressive properties compared to all other FGC cast and dry sprayed configurations used in this study. The compressive strength and energy absorption values are found to be higher for the FGC configurations with lower mixtures in the central layer compared to their counterparts. The crack is found to initiate in the weakest layer and propagate towards the highest density layers upon further loading.

The failure of the FGC cast configurations S3.3 and S3.4 emerge with horizontal cracks in the weakest layers. The lower density layer is being crushed while the ones with a higher strength remain undamaged. The cracking extends throughout the entire weak layer before the fracture propagates in the rest of the concrete cube. The stress-strain diagram has multiple peaks under large deformations. The failure is namely cascade graceful behaviour. The other FGC configurations, both cast and dry sprayed, initiate inclined cracks which delineates an hourglass-shaped compression core. The inclined cracks have a 60,...,90 degree angle for layers made of concrete with high tensile/compression strength and closer to 45,...,60 degree for those layers with lower tensile/compression strength, respectively. The failure is characterized by the axial splitting of the denser layer due to the secondary tensile stresses in the cube structure. The failure behaviour of all FGC configurations is characterized by unexpected large deformations.

Acknowledgements. The authors gratefully acknowledge the funding of this study by the German Research Foundation (DFG - Deutsche Forschungsgemeinschaft) as part of the Transregional Collaborative Research Centre (SFB/Transregio) 141 ‘Biological Design and Integrative Structures’/project A02.

REFERENCES

Bažant Z., *Concrete Fracture Models: Testing and Practice*. Engineering Fracture Mechanics, **69**, pp 165-205 (2002).

Bažant Z., Ožbolt J., *Compression Failure of Quasibrittle Material: Nonlocal Microplane Model*, Journal of Engineering Mechanics, **118(3)**, 540-556 (1992).

Bischoff P.H., Yamura K., Perry S.H., *Polystyrene Aggregate Concrete Subjected to Hard Impact*, In: Proceedings of the Institution of Civil Engineers, **89(2)**, London, 225-239 (1989).

Chi J.M., Huang R., Yang C.C., Chang J.J., *Effect of Aggregate Properties on the Strength and Stiffness of Lightweight Concrete*, Cem Concr Compos, **25(2)**, 197-205 (2003).

Green H., *Impact Strength of Concrete*, Proceedings of the Institution of Civil Engineers, **28**, London, 383-396 (1964).

Hasan N., Hashim S.F.S., Ariff Z.M., *The Influence Wall Thickness of Cement Hollow Spheres Towards Compressive Properties of Cement Syntactic Foam*, Advanced Materials Research, **701**, 291-295 (2013).

Huang J.-S., Huang Z.-H., *Fatigue of Cement Foams in Axial Compression*, Journal of Materials Science **35**, 4385-4391 (2000).

Klang K., Bauer G., Toader N., Lauer C., Termin K., Schmier S., Kovaleva D., Haase W., Berthold C., Nickel K. G., Speck T., Sobek W., *Plants and Animals as Source of Inspiration for Energy Dissipation in Load Bearing Systems and Facades* (chapter 7), In Knippers J, Speck T, Nickel K G (eds.) Biomimetic research for architecture and building construction. Springer International Publishing, 103-127 (2016).

Ravindrarajah R.S., Lyte M.C., *Energy Absorbing Concrete for Impact Loading*, Technical report of the Centre for Built Infrastructure Research, University of Technology, Sydney, 2007.

Toader N., Sobek W., Nickel K.G., *Energy Absorption in Functionally Graded Concrete Bioinspired by Sea Urchin Spines*, Journal of Bionic Engineering, **14(2)** (2017).

Yoon J.Y., Kim J.H., Hwang Y.Y., Shin D.K., *Lightweight Concrete Produced Using a Two-Stage Casting Process*, Materials, **8**, 1384-1397 (2015).

* * * *Eurocode 2: Design of concrete structures. Part 1–1: general rules and rules for buildings (EN 1992-1-1)*, CEN (Coomite Europeen de Normalization), Brussels, 2004.

ABSORPŢIA DE ENERGIE ÎN BETONUL CU GRADIENT DE DENSITATE SUPUS LA COMPRESIUNE

(Rezumat)

Elementele de rezistență din beton cu gradient de densitate se caracterizează printr-o distribuție internă a betonului de varii densități în funcție de magnitudinea tensiunilor interioare ce apar pentru o stare de solicitare dată. Astfel de elemente de rezistență au o capacitate portantă similară cu cea a elementelor cea au o distribuție omogenă a proprietăților betonului cu densitate normală (ordinară). Pentru specimenele din beton cu gradient de densitate se disting două tehnologii de fabricație: prin turnare şi prin torcretare uscată. Scopul este de a determina relația dintre alternarea straturilor de beton cu densități diferite şi cantitate de energie absorbită atunci când probele sunt supuse la compresiune uniaxială. Pentru evaluarea capacității absorpției de energie au fost fabricate cuburi de masă egală dar cu structură internă diferită. Rezultatele indică dependența capacității absorpției de energie în raport cu varierea structurii interne, precum şi cu tehnologia de fabricație utilizată.